Resummation of classical and semiclassical periodic-orbit formulas

Bruno Eckhardt* and Gunnar Russberg

Fachbereich Physik der Philipps-Universität, Renthof 6, D-3550 Marburg, Germany

(Received 20 August 1992; revised manuscript received 12 November 1992)

The convergence properties of cycle-expanded periodic-orbit expressions for the spectra of classical and semiclassical time evolution operators have been studied for the open three-disk billiard. We present evidence that the semiclassical and perhaps the classical Selberg zeta functions have poles. Applying a Padé approximation on the expansions of the full Euler products, as well as on the individual dynamical zeta functions in the products, we calculate the leading poles and the zeros of the improved expansions with the first few poles removed. The removal of poles tends to change the simple linear exponential convergence of the Selberg zeta functions to an $\exp\{-n^2\}$ decay in the semiclassical case. The classical Selberg zeta function decays like $\exp\{-n^{3/2}\}$. The leading poles of the jth dynamical zeta function are found to equal the leading zeros of the $(j+1)$th one: However, in contrast to the zeros, which are all simple, the poles seem without exception to be *double*. The poles are therefore in general *not* completely canceled by zeros in the way suggested by Artuso, Aurell, and Cvitanović [Nonlinearity 3, 325 (1990)]. The only complete cancellations of this kind occur in the classical Selberg zeta function between the poles (double) of the first and the zeros (squared) of the second dynamical zeta function. Furthermore, we find strong indications that poles are responsible for the presence of spurious zeros in periodic-orbit quantized spectra and that these spectra can be greatly improved by removing the leading poles, e.g., by using the Padé technique.

I. INTRODUCTION

Trace formulas in chaotic dynamical systems relate phase-space averages to sums over periodic orbits [1–6]. Exponential trace formulas give rise to Selberg-type zeta functions, named after corresponding expressions arising in studies of billiards on surfaces of negative curvature [7,8]. Selberg zeta functions factorize further into products of dynamical zeta functions, each one being an infinite product over all primitive nonrepeated periodic orbits (PPO) of the system. Finally, the term cycle expansion refers to a certain expansion and truncation of (dynamical and Selberg) zeta functions into polynomials. Whereas the original trace formulas and the infinite products have the same convergence and analyticity properties, cycle-expanded periodic-orbit expressions typically converge much better [3,4].

Calculations can be improved if the pole structure is known [9]. Typically, dynamical zeta functions will have poles; for Selberg zeta functions, one can advance arguments [3,10] that they should be entire and thus ideally suited for numerical purposes. We present here quantitative results on the analyticity properties of zeta functions for a two-dimensional (2D) conservative dynamical system, a point particle elastically scattered off three disks placed symmetrically in the plane [11–14]. This system is ideally suited for such an investigation since (for sufficiently separated disks) it is a hyperbolic system with a good symbolic coding (complete binary, once the symmetries are factored out). Periodic orbits can conveniently and accurately be computed.

We proceed with a formal definition of the objects investigated: Let p denote all primitive nonrepeated

periodic orbits, n_p their symbolic length, μ_p the Maslov index (in a billiard $\mu_p = 2n_p$), and J_p the linearization perpendicular to the orbit, with Λ_p the eigenvalue of largest absolute value. For the two-degree-of-freedom system considered here J_p is a 2×2 matrix of determinant 1 so that the other eigenvalue is $1/\Lambda_p$. We then consider the classical Selberg zeta function [5]

$$Z(z) = \exp\left\{-\sum_p \sum_{r=1}^{\infty} \frac{z^{rn_p}}{r} \frac{1}{|\det(1-J_p^r)|}\right\}$$
$$= \prod_{j=0}^{\infty} [\zeta_j^{-1}(z)]^{j+1},\tag{1}$$

with

$$\zeta_j^{-1}(z) = \prod_p (1-z^{n_p}|\Lambda_p|^{-1}\Lambda_p^{-j}),\tag{2}$$

and the semiclassical Selberg zeta function [15–17]

$$Z(z) = \exp\left\{-\sum_p \sum_{r=1}^{\infty} \frac{z^{rn_p}}{r} \frac{e^{-ir\mu_p\pi/2}}{|\det(1-J_p^r)|^{1/2}}\right\}$$
$$= \prod_{j=0}^{\infty} \zeta_j^{-1}(z)\tag{3}$$

with

$$\zeta_j^{-1}(z) = \prod_p (1-z^{n_p}e^{-i\mu_p\pi/2}|\Lambda_p|^{-1/2}\Lambda_p^{-j}),\tag{4}$$

all as functions of z. We avoid use of additional labels distinguishing classical and semiclassical zeta functions and hope that it is clear from the context which one is meant. Straightforward formal manipulations allow to

express each function (1)–(4) as a power series $\sum_n C_n z^n$ in z, which, when truncated, yields the cycle expansion. Where needed, we will abbreviate with t_p the contributions of periodic orbits to the dynamical zeta function with $j = 0$ so that $\zeta_j^{-1} = \prod_p (1 - t_p \Lambda_p^{-j})$.

The above expressions are correct for maps, the periods of orbits being integers. For flows one would replace z^{n_p} by $z^{n_p} \exp\{i \omega T_p\}$ in the classical case or by $z^{n_p} \exp\{i S_p(E)/\hbar\}$ in the semiclassical case, expand in a power series in z, and consider the final result as a function of frequency ω or energy E, respectively, for $z = 1$. In billiards, the action is given by $S_p(E)/\hbar = L_p k(E)$, where L_p is the geometrical length of the PPO and $k(E) = \sqrt{2mE}/\hbar$ is the wave number. In addition to Maslov phases there can be further phases due to symmetries [18–20]. For the case of three disks, the above expressions are correct in the A_1 subspace; in the A_2 subspace there is an additional phase $i\pi$ if n_p is odd.

Periodic orbits for the three-disk system have been computed using Newton's method on two different maps, one based on direct description (impact parameter, scattering angle) of collisions with the disks and one based on stationarity of action. The computations were done for several values of the ratio $\rho \equiv d/R$, where d is the disk separation and R the disk radius. Symmetry-reduced orbits up to symbolic length 13 have been found in double-precision numerics with relative accuracy 10^{-14}. The exponential of (1) and (3) was computed using all orbits and repetitions satisfying $n_p r \leq N$ and then expanded in a series $\sum_n C_n z^n$ using the recurrence relations of Plemelj [21] and Smithies [22] (see also Ref. [23]).

Figure 1 shows the results for the classical Selberg zeta function. An apparently faster-than-exponential decay is observed. In contrast, the semiclassical Selberg zeta function seems to decay faster than exponentially for the first three or four terms, but then settles for an exponential decay; see Fig. 2. In the following we will explain this difference in behavior, show its effects in calculations, and demonstrate how this knowledge can be used to improve calculations.

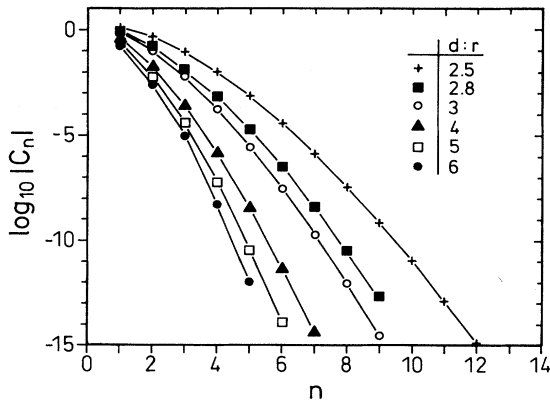We begin in Sec. II with a detailed discussion of the

FIG. 1. Expansion coefficients C_n of the classical Selberg zeta function (1) for different d/R in the open three-disk system. (A_1 subspace.)
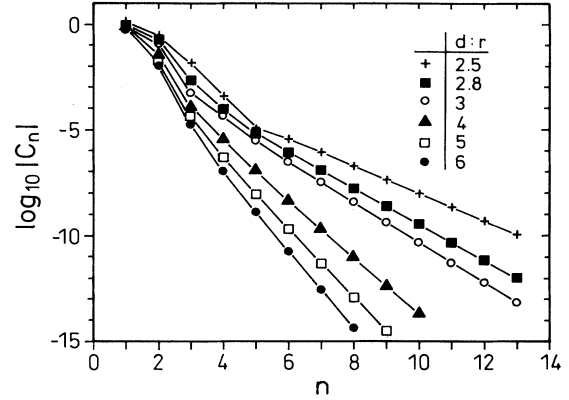

FIG. 2. Expansion coefficients C_n of the semiclassical Selberg zeta function (3) for different d/R in the open three-disk system. (A_1 subspace.)

convergence of cycle-expanded zeta functions, including numerical results for the three-disk system. In Sec. III we turn to methods for identification and removal of poles. The effect of poles when calculating quantum resonances is discussed in Sec. IV. We conclude with a short summary and comments on other systems in Sec. V.

II. CONVERGENCE ESTIMATES

Some insight into the behavior of the cycle expansions of (1) and (3) may be obtained by considering the special case of a complete binary code with $\Lambda_0 \sim \Lambda_1 \sim \Lambda$ and a factorization of the eigenvalues of the longer periodic orbits $\Lambda_p \sim \Lambda_0^{n_0} \Lambda_1^{n_1}$, where n_0 and n_1 are the numbers of zeros and ones in the symbolic description of p. Then the classical dynamical zeta functions take on the form

$$\zeta_j^{-1}(z) \sim (1 - 2z |\Lambda|^{-1} \Lambda^{-j}) . \tag{5}$$

Expanding the product on j in a power series in z, one finds

$$Z(z) = \prod_j [\zeta_j^{-1}(z)]^{j+1} \sim \sum_n d_n z^n , \tag{6}$$

with $d_n \sim \Lambda^{-n^{3/2}}$ (see below). Similarly, in the semiclassical case one finds

$$\zeta_j^{-1}(z) \sim (1 - 2z |\Lambda|^{-1/2} \Lambda^{-j}) \tag{7}$$

and

$$Z(z) = \prod_j \zeta_j^{-1}(z) \sim \sum_n d_n' z^n , \tag{8}$$

with $d_n' \sim \Lambda^{-n^2}$ [essentially due to the Euler product formula; see, e.g., Eq. (89.18.3) in Ref. [24]]. Because of this rapid decay, these functions are free of poles.

In the general hyperbolic case, the expansion of dynamical zeta functions does not stop with the linear term but rather continues with exponentially decaying coefficients, $c_n \sim \beta^n$ with $|\beta| < 1$. Summing this geometrical series one finds a pole at $z = \beta^{-1}$. In Refs. [3,10], β has been related to the Lyapunov exponents which suggests that the poles of ζ_j^{-1} should be compensated by the

zeros of ζ_{j+1}^{-1}. To see what terms have to compensate in order to provide faster-than-exponential decay of the coefficients in the Selberg-type zeta function, let us consider the classical and semiclassical cases in more detail.

A. Semiclassical case

With each dynamical zeta function expanded in a power series in z, the semiclassical Selberg zeta function (3) looks like

$$
\begin{aligned}
Z(z) &= \prod_j \zeta_j^{-1}(z) \\
&= (1 - f_1^{(0)}z - c_6^{(0)}z^2 - c_9^{(0)}z^3 - \cdots) \\
&\quad \times (1 - f_3^{(1)}z - c_{10}^{(1)}z^2 - \cdots) \\
&\quad \times (1 - f_5^{(2)}z - c_{14}^{(2)}z^2 - \cdots) \cdots .
\end{aligned}
\tag{9}
$$

As is often convenient for dynamical zeta functions we distinguish curvature terms c_{i_n} of orbits grouped together with shorter shadowing orbits and fundamental contributions f_i of the shortest orbits, which by definition are not approximated by other orbits. Superscript labels here indicate the order j of the zeta function. Subscripts indicate the size of the terms in powers of $|\Lambda|^{-1/2}$, where $|\Lambda|$ is a typical instability of the shortest orbits (obviously, some uniformity in the Lyapunov exponents is assumed here). For instance, $f_1^{(0)}$ comes from terms of the form $|\Lambda_p|^{-1/2}e^{-i\mu_p\pi/2}$ in ζ_0^{-1}, whence its subscript equals 1. Fundamentals $f_i^{(j)}$ with higher j have additional powers $|\Lambda_p|^{-j}$ and thus $i = 1 + 2j$. The order of the curvature corrections $c_{i_n}^{(j)}z^n$ is determined by two factors: the typical size of the terms contributing (about $|\Lambda|^{-n/2 - jn}$) and an additional factor $\sim \Lambda^{-n}$ due to exponential shadowing of long orbits by short approximants; thus $i_n = (3 + 2j)n$.

To estimate the convergence behavior, we will now expand (9) in z, $Z(z) = \sum_n C_n z^n$, and evaluate the leading-order contributions in each coefficient C_n. One sees that there is a considerable difference in order of magnitude between the fundamental term and the first curvature correction, so to begin with one would expect to find significant contributions from fundamentals only. In the ideal two-scale approximation $\Lambda_p = \Lambda_0^{n_0}\Lambda_1^{n_1}$ all curvatures are identically zero, $c_{i_n}^{(j)} = 0$, and the expansion looks as follows:

$$
\begin{aligned}
Z(z) &= (1 - f_1^{(0)}z)(1 - f_3^{(1)}z)(1 - f_5^{(2)}z) \cdots \\
&= 1 - (f_1^{(0)} + f_3^{(1)} + f_5^{(2)} + \cdots)z + (f_1^{(0)}f_3^{(1)} + f_1^{(0)}f_5^{(2)} + f_1^{(0)}f_7^{(3)} + f_3^{(1)}f_5^{(2)} + \cdots)z^2 \\
&\quad - (f_1^{(0)}f_3^{(1)}f_5^{(2)} + f_1^{(0)}f_3^{(1)}f_7^{(3)} + \cdots)z^3 + \cdots \\
&\equiv \sum_{n=0}^{\infty} d_n' z^n .
\end{aligned}
\tag{10}
$$

We notice that the leading terms grow in order (I_n) like $I_2 = 1$, $I_2 = 1 + 3 = 4$, $I_3 = 1 + 3 + 5 = 9, \ldots$, i.e., $\ln d_n' \sim I_n = \sum_{j=0}^{n-1}(1 + 2j) = n^2$, a quadratic exponential convergence.

In the full evaluation of (9) we cannot expect the purely fundamental product terms to be leading forever. Arranging products as above according to the sum of the lower indices and calling the leading fundamental terms F_{n^2} we find the following expansion coefficients C_n:

$$
\begin{aligned}
C_0 &= 1 , \\
C_1 &= F_1 - f_3^{(1)} - f_5^{(2)} + O(7) , \\
C_2 &= F_4 + f_1^{(0)}f_5^{(2)} - c_6^{(0)} + f_1^{(0)}f_7^{(3)} + f_3^{(1)}f_5^{(2)} \\
&\quad - c_9^{(0)} + O(10) , \\
C_3 &= F_9 - c_9^{(0)} + f_3^{(1)}c_6^{(0)} - f_1^{(0)}f_3^{(1)}f_7^{(3)} + f_5^{(2)}c_6^{(0)} \\
&\quad + f_1^{(0)}c_{10}^{(1)} + O(12) , \\
C_4 &= -c_{12}^{(0)} + f_3^{(1)}c_9^{(0)} + f_5^{(2)}c_9^{(0)} - f_3^{(1)}f_5^{(2)}c_6^{(0)} \\
&\quad + F_{16} + f_1^{(0)}c_{15}^{(1)} + \cdots + O(18) , \\
C_5 &= -c_{15}^{(0)} + f_3^{(1)}c_{12}^{(0)} + f_5^{(2)}c_{12}^{(0)} - f_3^{(1)}f_5^{(2)}c_9^{(0)} \\
&\quad + \cdots + F_{25} + \cdots + O(27) ,
\end{aligned}
\tag{11}
$$

etc., where $O(n)$ indicates terms of size $\sim \Lambda^{-n}$. Up to and including $n = 3$ the convergence is unconditionally quadratic as in the ideal situation. At larger n, however, due to the simple exponential decay of the pure curvatures, these as well as mixed curvature and fundamental cross product terms have outgrown the pure fundamental ones. Unless there now exist efficient additional cancellations within complexes of the form

$$
c_{3n}^{(0)} - f_3^{(1)}c_{3n-3}^{(0)} ,
\tag{12}
$$

raising their order to at least n^2, a sudden change in the convergence behavior of the semiclassical Selberg zeta function around $n = 4$ is to be expected. This is indeed what is observed in Fig. 2.

B. Classical case

Following the procedure in the semiclassical treatment above we now analyze the slightly more complicated classical Selberg zeta function (1),

$$
\begin{aligned}
Z(z) &= \prod_j [\zeta_j^{-1}(z)]^{j+1} \\
&= (1 - f_1^{(0)}z - c_4^{(0)}z^2 - c_6^{(0)}z^3 - \cdots) \\
&\quad \times (1 - f_2^{(1)}z - c_6^{(1)}z^2 - \cdots)^2 \\
&\quad \times (1 - f_3^{(2)}z - c_8^{(2)}z^2 - \cdots)^3 \cdots .
\end{aligned}
\tag{13}
$$

Since in the classical case weights are proportional to powers of $|\Lambda_p|^{-1}$, subscripts now indicate the size of the terms in powers of $|\Lambda|^{-1}$ rather than $|\Lambda|^{-1/2}$.

The convergence behavior in the ideal case $c_{i_n}^{(j)} = 0$ is found as follows: From a straightforward expansion of

$$Z(z) = (1 - f_1^{(0)} z)(1 - f_2^{(1)} z)^2 (1 - f_2^{(2)} z)^3 \cdots$$

$$\equiv \sum_{n=0}^{\infty} d_n z^n , \tag{14}$$

one obtains the expansion coefficients

$$
\begin{aligned}
d_0 &= 1 , \\
d_1 &= -f_1^{(0)} + \cdots = O(1) , \\
d_2 &= 2 f_1^{(0)} f_2^{(1)} + \cdots = O(3) , \\
d_3 &= -f_1^{(0)} f_2^{(1)} f_2^{(1)} + \cdots = O(5) , \\
d_4 &= 3 f_1^{(0)} f_2^{(1)} f_2^{(1)} f_3^{(2)} + \cdots = O(8) , \\
d_5 &= -3 f_1^{(0)} f_2^{(1)} f_2^{(1)} f_3^{(2)} f_3^{(2)} + \cdots = O(11) , \\
d_6 &= f_1^{(0)} f_2^{(1)} f_2^{(1)} f_3^{(2)} f_3^{(2)} f_3^{(2)} + \cdots = O(14) , \\
d_7 &= -4 f_1^{(0)} f_2^{(1)} f_2^{(1)} f_3^{(2)} f_3^{(2)} f_3^{(2)} f_4^{(3)} + \cdots = O(18) ,
\end{aligned}
\tag{15}
$$

etc. The growth rule should be obvious: From the jth zeta function (counting ζ_0^{-1} as the first), there are j consecutive contributions to the leading-order terms, each increasing the order of magnitude by an amount j, i.e., $j = j_n$ grows by one over an interval of length $\Delta n = j_n$ and the total growth in order I_n is $\Delta I_n = I_{n+\Delta n} - I_n = j_n^2$. For large n one thus ends up with the following differential equations:

$$\frac{dn}{dj} = j , \tag{16}$$

$$\frac{dI}{dn} = j . \tag{17}$$

Equation (16) gives $j_n = n^{1/2}$, which is inserted into Eq. (17). The solution of the resulting equation is the sought-after asymptotic relation $I_n \sim n^{3/2}$.

The full evaluation of Eq. (13) gives

$$
\begin{aligned}
C_0 &= 1 , \\
C_1 &= F_1 - 2 f_2^{(1)} - 3 f_3^{(2)} + O(4) , \\
C_2 &= F_3 - c_4^{(0)} - f_2^{(1)} f_2^{(1)} + 3 f_1^{(0)} f_3^{(2)} + 6 f_2^{(1)} f_3^{(2)} \\
&\quad + 4 f_1^{(0)} f_4^{(3)} + O(6) , \\
C_3 &= F_5 - c_6^{(0)} + 2 f_2^{(1)} c_4^{(0)} - 6 f_1^{(0)} f_2^{(1)} f_3^{(2)} + 2 f_1^{(0)} c_6^{(1)} \\
&\quad + 3 f_3^{(2)} c_4^{(0)} - \cdots + O(8) , \\
C_4 &= F_8 - c_8^{(0)} + 2 f_2^{(1)} c_6^{(0)} - f_2^{(1)} f_2^{(1)} c_4^{(0)} - 2 f_1^{(0)} f_2^{(1)} c_6^{(1)} \\
&\quad + 3 f_3^{(2)} c_6^{(0)} + \cdots + O(10) , \\
C_5 &= -c_{10}^{(0)} + 2 f_2^{(1)} c_8^{(0)} - f_2^{(1)} f_2^{(1)} c_6^{(0)} + F_{11} + \cdots + O(12) ,
\end{aligned}
\tag{18}
$$

etc. The leading-order terms in each C_n which have to compensate in order to get the faster than exponential convergence $n^{3/2}$ are now of the form

$$c_{2n}^{(0)} - 2 f_2^{(1)} c_{2n-2}^{(0)} + f_2^{(1)} f_2^{(1)} c_{2n-4}^{(0)} . \tag{19}$$

Things work out nicely until order 4; beginning from order 5 additional cancellations are needed. As Fig. 1 shows, these seem to occur in the classical case.

C. Numerical estimate of curvatures

A rather crude estimate of the *individual* curvature terms $c_p^{(j)} \sim t_p \Lambda_p^{-(j+1)}$, where $t_p = |\Lambda_p|^{-1}$ in the classical and $t_p = |\Lambda_p|^{-1/2}$ in the semiclassical case, was used above to obtain the correct order of magnitude for the *full* curvatures $c_{i_n}^{(j)}$, each being a sum over individuals with the same symbol length. One would benefit more from the results of the preceding sections if there were a better estimate of the individual curvatures $c_p^{(0)}$ in ζ_0^{-1}. Consider again a system with binary symbolic dynamics.

First note that due to uncertainty in the building of complexes like $c_{00011}^{(0)} = t_{00011} - t_{0001} t_1 - t_0 t_{0011} + t_0 t_{001} t_1$ and $c_{00101}^{(0)} = t_{00101} - t_{001} t_{01}$ it appears necessary to collect curvatures with the same number of zeros and ones into a single term,

$$c_{nm} \equiv \sum_p \delta_{n,n_0} \delta_{m,n_1} c_p^{(0)} , \tag{20}$$

where the Kronecker deltas select primitive periodic orbits with number of symbols $n_0 = n$ and $n_1 = m$. After this precaution one may make the following ansatz,

$$c_{n_0 n_1} \equiv \alpha_{n_0 n_1} (t_0 \Lambda_0^{-1})^{n_0} (t_1 \Lambda_1^{-1})^{n_1} , \tag{21}$$

hoping that the essential stability dependence has been correctly extracted, so that the prefactors $\alpha_{n_0 n_1}$ depend only weakly on stability. We aim at finding an approximation for the prefactors $\alpha_{n_0 n_1}$ better than $\alpha_{n_0 n_1} \sim 1$.

We have calculated the prefactors $\alpha_{n_0 n_1}$ up to symbol length 6 for the open three-disk system, with values of ρ $(=d/R)$ ranging from 2.5 to 6.0, and with weights given by $t_p = |\Lambda_p|^{-D}$. The results of the calculations are presented in Table I ($D = \frac{1}{2}$, semiclassical case) and Table II ($D = 1$, classical case). The values for $D = 1$ are roughly twice those for $D = \frac{1}{2}$ and some variation in parallel with the instabilities Λ_0 and Λ_1 is noticeable. The dependence on n_0 and n_1 seems to be roughly binomial with an additional factor $n_0 + n_1$; we conclude that the data in Tables I and II should be more or less well approximated by the following formula:

$$\alpha_{n_0 n_1} \approx D h_D(\Lambda_0(\rho), \Lambda_1(\rho))(n_0 + n_1) \begin{bmatrix} n_0 + n_1 - 2 \\ n_0 - 1 \end{bmatrix}$$

$$\equiv D \tilde{h}_D(\rho) B_{n_0 n_1} , \tag{22}$$

where h_D captures the dependence on the separation ratio ρ. Figure 3 shows the rescaled prefactors $\alpha_{n_0 n_1} / D B_{n_0 n_1}$ as a function of ρ, together with the linear fits of the data:

$$\tilde{h}_1(\rho) \approx -0.584 + 0.378 \rho , \tag{23}$$

$$\tilde{h}_{1/2}(\rho) \approx -0.506 + 0.376 \rho . \tag{24}$$

TABLE I. Semiclassical curvature prefactors α_{n_0,n_1} of ζ_0^{-1} [Eq. (4)] for the open three-disk system (A_1 subspace).

	d/R					
	2.5	2.8	3.0	4.0	5.0	6.0
Λ_0	2.6180	3.2967	3.7321	5.8284	7.8730	9.8990
$-\Lambda_1$	3.4867	4.2299	4.7162	7.0967	9.4411	11.771
α_{11}	1.1186	1.3544	1.5062	2.2298	2.9255	3.6098
α_{21}	1.6744	2.0904	2.3410	3.4572	4.4835	5.4784
α_{12}	1.1115	1.4729	1.7097	2.8696	4.0094	5.1394
α_{31}	2.0462	2.6014	2.9302	4.3757	5.7007	6.9875
α_{22}	3.0188	4.0646	4.7274	7.8445	10.811	13.713
α_{13}	1.6862	2.1916	2.5191	4.1148	5.6864	7.2505
α_{41}	2.3333	3.0303	3.4400	5.2285	6.8635	8.4507
α_{32}	5.3147	7.2931	8.5355	14.296	19.712	24.989
α_{23}	5.6405	7.5660	8.7926	14.659	20.352	25.982
α_{14}	2.0389	2.7079	3.1391	5.2205	7.2543	9.2723
α_{51}	2.6004	3.4420	3.9340	6.0712	8.0196	9.9093
α_{42}	7.8084	10.979	12.964	22.091	30.607	38.877
α_{33}	11.894	16.481	19.395	33.237	46.568	59.695
α_{24}	8.4893	11.638	13.651	23.287	32.652	41.925
α_{15}	2.4947	3.3024	3.8249	6.3585	8.8413	11.307

The relative deviations from the linear fits are rather large for small values of ρ, but shrink with increasing ρ; at $\rho = 6$ the maximum relative error is less than 10% (semiclassical case). The ansatz $h_D(\Lambda_0, \Lambda_1) \approx \kappa_D |\Lambda_0 \Lambda_1|^{1/2}$ with $\kappa_1 \approx \kappa_{1/2} \approx 0.2$ is another simple and relatively accurate estimate.

Equation (22) gives us information with sufficient detail that we may now return to the question of whether there exist additional cancellations in the classical and semiclassical cycle expansions for the open three-disk problem. The estimate of the full curvatures becomes

$$c_{i_n}^{(0)} \approx nDh_D \sum_{n_0=1}^{n-1} \begin{bmatrix} n-2 \\ n_0-1 \end{bmatrix} \lambda_0^{n_0} \lambda_1^{n-n_0}$$

$$= nDh_D \lambda_0 \lambda_1 (\lambda_0 + \lambda_1)^{n-2}$$

$$= nDh_D \lambda_0 \lambda_1 f_D^{n-2}, \tag{25}$$

where f_D refers to $f_2^{(1)}$ in the classical and $f_3^{(1)}$ in the semiclassical case, respectively. For short, we have written $\lambda_0 \equiv t_0 \Lambda_0^{-1}$ and $\lambda_1 \equiv t_1 \Lambda_1^{-1}$. The perhaps surprising observation to emerge from Eq. (25) is that the leading

TABLE II. Classical curvature prefactors α_{n_0,n_1} of ζ_0^{-1} [Eq. (2)] for the open three-disk system (A_1 subspace).

|	d/R					
	2.5	2.8	3.0	4.0	5.0	6.0
α_{11}	2.1001	2.5773	2.8835	4.3394	5.7359	7.1077
α_{21}	2.8211	3.6797	4.1979	6.4921	8.5797	10.591
α_{12}	1.9894	2.6964	3.1619	5.4579	7.7261	9.9797
α_{31}	3.2373	4.4162	5.1151	8.1406	10.858	13.471
α_{22}	4.7872	6.8163	8.1208	14.328	20.266	26.080
α_{13}	3.0514	4.0477	4.6946	7.8584	10.985	14.103
α_{41}	3.5819	5.0739	5.9509	9.7075	13.063	16.287
α_{32}	7.6837	11.527	13.990	25.561	36.474	47.090
α_{23}	9.1325	12.845	15.236	26.806	38.119	49.337
α_{14}	3.6692	4.9844	5.8351	9.9614	14.009	18.032
α_{51}	3.9392	5.7353	6.7861	11.267	15.262	19.097
α_{42}	10.575	16.709	20.651	39.052	56.258	72.928
α_{33}	17.569	26.216	31.833	59.045	85.552	111.74
α_{24}	13.644	19.669	23.571	42.501	61.064	79.508
α_{15}	4.4981	6.0848	7.1147	12.135	17.074	21.988
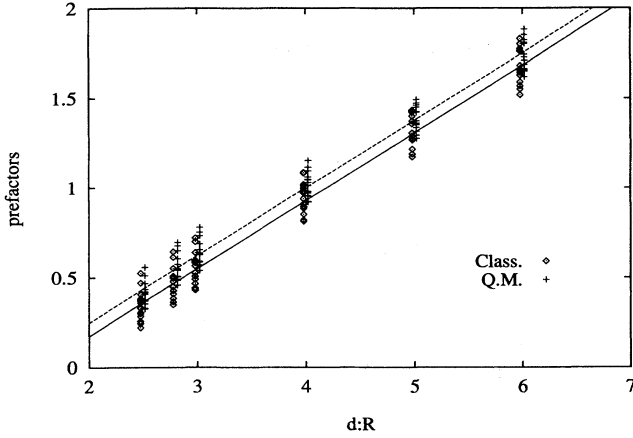
FIG. 3. Rescaled semiclassical (diamonds) and classical (crosses) curvature prefactors $\alpha_{n_0 n_1}/DB_{n_0 n_1}$ for different ρ $(=d/R)$ in the A_1 subspace. The straight lines are the corresponding linear approximations [Eq. (24)]: $\tilde{h}_{1/2}(\rho)$ in the semiclassical case (dashed line), and $\tilde{h}_1(\rho)$ in the classical case (solid line).

pole of $\zeta_0^{-1}(z)$ has to be double:

$$\sum_n c_{i_n}^{(0)} z^n = Dh_D \lambda_0 \lambda_1 f_D^{-1} z \sum_n n (f_D z)^{n-1} \sim \frac{z}{(1-f_D z)^2} \ .$$

$$(26)$$

If (25) is now inserted into the semiclassical complexes (12),

$$c_{i_n}^{(0)} - f_D c_{i_{n-1}}^{(0)} \approx [n-(n-1)] Dh_D \lambda_0 \lambda_1 f_D^{n-2}$$

$$= Dh_D \lambda_0 \lambda_1 f_D^{n-2} \neq 0 \ , \qquad (27)$$

the terms do not cancel; there still remains a rest of (roughly) order $O(3n)$, building up a (simple) pole at $z_p = 1/f_3^{(1)} = (|\Lambda_0|^{-1/2}\Lambda_0^{-1} + |\Lambda_1|^{-1/2}\Lambda_1^{-1})^{-1}$. This is in line with our earlier numerical findings that the semiclassical Selberg zeta function is not free of poles. However, if we insert the same expression (25) into the classical complexes (19),

$$c_{i_n}^{(0)} - 2f_D c_{i_{n-1}}^{(0)} + f_D^2 c_{i_{n-2}}^{(0)}$$

$$\approx [n - 2(n-1) + (n-2)] Dh_D \lambda_0 \lambda_1 f_D^{n-2} = 0 \ , \qquad (28)$$

the additional cancellations are there.

Note that the qualitative results above are independent of the choice of weight (i.e., the values of D); the different results for the classical and the semiclassical Selberg zeta function are entirely due to the difference in the power of ζ_1^{-1}. The double pole of ζ_0^{-1} occurs at $z_p \approx f_D^{-1}$, which is identical to the lowest-order approximation of the leading zero of $\zeta_1^{-1}(z)$. By taking the square of $\zeta_1^{-1}(z)$ as in the classical Selberg zeta function one doubles the leading zero, which then precisely cancels the double pole of ζ_0^{-1}. In the semiclassical case the simple zero of ζ_1^{-1} cancels only one pole with a simple pole remaining [Eq. (27)]. We study this point further below.

The conjecture [3] that the position of the poles of the dynamical zeta function ζ_j is given by the zeros of ζ_{j+1} remains valid, but the order of the poles is not simple but double. Returning to the arguments of Aurell and co-workers [3,10] one notes that they are rather liberal with the prefactors, and it is precisely in the prefactors that the difference between a simple and a double pole resides.

III. IDENTIFICATION AND REMOVAL OF POLES

In the case of maps, phase-space averages can be related to zeros of zeta functions $Z(z) = \sum_{n=0}^{\infty} C_n z^n$. Practical calculations estimate such zeros from a truncation of the series, $F_N(z) = \sum_{n=0}^{N} C_n z^n$. In ideal situations, exponential [3,4] or even faster-than-exponential convergence [9] is obtained. The presence of poles destroys faster than exponential convergence and makes it more difficult to calculate the exact positions of the zeros; consider a simple case where there is one zero and one pole:

$$F(z) = \frac{1-az}{1-bz} = (1-az)(1+bz+b^2 z^2 + \cdots)$$

$$= 1 - (a-b)z - (a-b)bz^2 - \cdots = \sum_{n=0}^{\infty} C_n z^n \ . \qquad (29)$$

We assume that $0 < b < a$. A truncation after the linear term gives a value of the zero $z_0' = (a-b)^{-1}$. This is obviously a bad estimate of the true value $z_0 = a^{-1}$ if a and b are of the same order of magnitude. The inclusion of higher-order terms only slowly improves z_0', the error being $\sim (b/a)^N$ asymptotically. Furthermore, additional "ghost" zeros appear: The number of these unwanted zeros equals $N-1$ and they do not vanish to infinity as N grows large—they cluster around the circle $|z| = b^{-1}$, which borders the region of absolute convergence. To see this, consider the function

$$\tilde{F}_N(z) = \frac{(1-az)[1-(bz)^N]}{1-bz} = (1-az) \sum_{j=0}^{N-1} (bz)^j \ , \qquad (30)$$

which differs from $F_N(z)$ only in the coefficient C_N. It clearly has $N-1$ additional zeros on the circle $|z| = b^{-1}$. For $b > a > 0$ the situation is still worse; there is *no* zero of $F_N(z)$ converging to $z_0 = a^{-1}$.

If on the other hand the pole were absent, one would have a polynomial $1-az$, which "converges" to its exact form already after the first term in the "expansion"; the zero $z_0 = a^{-1}$ is at once correctly determined. By estimating the value of b from the asymptotic behavior of the coefficients C_n, we could remove the effect of the pole: Assume an estimate $\tilde{b}$ close to b with $|b - \tilde{b}| = |\varepsilon| \ll a$. Then the function

$$(1-\tilde{b}z)F(z) = 1 - (a-\varepsilon)z$$

$$-\varepsilon(a-b)z^2[1+bz+b^2 z^2 + \cdots] \qquad (31)$$

has already in the linear approximation a zero $\tilde{z}_0 = (a-\varepsilon)^{-1}$ close to z_0. The position of the ghost zeros may be estimated from the function [cf. Eq. (30)]

TABLE III. Leading zeros and poles of the semiclassical Selberg zeta function (3) and of the three lowest-order dynamical zeta functions (4) in the A_1 subspace, determined from the different Padé approximations of the respective functions ($N \leq 13$).

d/R	z zero	z pole	ζ_0^{-1} zero	ζ_0^{-1} pole	ζ_1^{-1} zero	ζ_1^{-1} pole	ζ_2^{-1} zero	ζ_2^{-1} pole
2.5	0.901 776	4.477...	0.901 776	4.48...	4.477 109	8.904 1...	8.904 120	29.31...
2.8	0.992 814	6.978...	0.992 814	6.979...	6.979 119	14.706 24	14.706 24	68.4...
3.0	1.048 112	8.917...	1.048 112	8.917...	8.917 864	19.418 66	19.418 66	108.7...
4.0	1.285 008	21.88...	1.285 008	21.86...	21.878 53	54.551 28	54.551 28	592...
5.0	1.481 805	40.2...	1.481 805	39.9...	40.175 55	111.762 7	111.762 7	1876...
6.0	1.654 411	63.6...	1.654 411	63.3...	63.590 37	194.356 8	194.356 8	4508...

$$(1 - \tilde{b}z)\tilde{F}_N(z) = (1 - az)\left[1 + (\varepsilon/b)\sum_{j=1}^{N}(bz)^j\right]; \qquad (32)$$

for large z, it is dominated by the highest power of z, so that its zeros lie on the circle $|z| \sim (\varepsilon/b)^{-1/N}b^{-1}$. They tend to infinity as $\varepsilon \to 0$.

If several poles are present, as, e.g., in a rational function

$$F(z) = \frac{P(z)}{Q(z)}, \qquad (33)$$

with polynomials P and Q, the zeros $|z_1| \ll |z_2| \ll |z_3| \ll \cdots$ of Q being different from the zeros of P, the removal of the leading pole z_1 leaves a function where z_2 determines the convergence. In the special case $P(z) = (1 - az)$ and $Q(z) = (1 - b_1 z)(1 - b_2 z)$ with $0 < b_2 \ll b_1 < a$, the removal of $z_1 = b_1^{-1}$ pushes the ghost zeros to the neighborhood of $|z| = b_2^{-1}$ and the error in the linear estimate of z_0 shrinks from $b_1[a(a - b_1)]^{-1}$, which may be larger than a^{-1}, to $b_2[a(a - b_2)]^{-1} \ll a^{-1}$. If z_2 in the last example is not much larger than z_1, but close in magnitude, the improvement is of course only marginal. Thus if two (or n) leading poles are close in magnitude, one has to remove both (all n) before any considerable improvement takes place.

To remove a certain number of poles in a consistent way, one may use a Padé approximation [25]: Assume that $N + 1$ coefficients C_n of the function $F(z) = P(z)/Q(z) = \sum_{n=0}^{N} C_n z^n$ are known and that one wants to know the power-series expansion of the unknown functions $P_M(z) = \sum_{n=0}^{M} A_n z^n$ and $Q_L(z) = \sum_{n=0}^{L} B_n z^n$. With the normalization $B_0 = 1$, one has to determine $M + 1 + L$ coefficients A_n, B_n, so that $N = M + L$ is required. The coefficients are determined

from $Q_L(z)F_N(z) = P_{N-L}(z)$, i.e.,

$$\sum_{n=0}^{N}\sum_{n'=0}^{L}\Theta(N - n - n')C_n B_{n'} z^{n+n'} = \sum_{n=0}^{N-L} A_n z^n;$$

$$\Theta(x) \equiv \begin{cases} 0, & x < 0 \\ 1, & x \geq 0. \end{cases} \qquad (34)$$

By identifying terms of equal power in z, one finds altogether $N + 1$ equations for the $M + L + 1 = N + 1$ unknowns.

Once the coefficients are known, the solution of $Q_L(\tilde{z}_p) = 0$ gives approximately the position(s) of the dominant pole(s). If the computed value $\tilde{z}_p$ converges for increasing L (and N), one may feel confident about really having identified a pole. Similarly, solutions of $P_M(\tilde{z}_0) = 0$ that converge for increasing L and N should give improved estimates of the zeros of the full function $F(z)$. (Calculating poles is in general much more difficult than finding good values for the zeros; even the leading pole requires large N.)

We have applied this to the three-disk system. An approximation with linear denominator $Q_1(z)$ already gave good results, confirmed and stabilized by computations for quadratic and higher-order denominators. The positions of the leading zeros and poles of the full Selberg zeta function and of the three first dynamical zeta functions are listed in Tables III–VI. The data clearly confirm the conclusion drawn at the end of the preceding section that the poles of ζ_j^{-1} approximately coincide with zeros of ζ_{j+1}^{-1}. The poles appeared in the computations either as pairs of nearby real values or as pairs of complex-conjugate values with small imaginary parts, a strong indication that they are double. Assuming that they are all real and double, the identification of poles

TABLE IV. Zeros and poles of the semiclassical zeta functions in the A_2 subspace. (cf. Table III).

d/R	z zero	z pole	ζ_0^{-1} zero	ζ_0^{-1} pole	ζ_1^{-1} zero	ζ_1^{-1} pole	ζ_2^{-1} zero	ζ_2^{-1} pole
2.5	−1.903 081	−2.883 523	−1.903 081	−2.883 523	−2.883 523	−11.339...	−11.336 765	−26.12...
2.8	−2.478 382	−3.864 797	−2.478 382	−3.864 797	−3.864 797	−21.5005...	−21.500 63	−54.290...
3.0	−2.867 599	−4.554 415	−2.867 599	−4.554 415	−4.554 415	−30.5791...	−30.579 32	−80.822...
4.0	−4.888 079	−8.421 929	−4.888 079	−8.421 928	−8.421 929	−111.00...	−111.006 1	−348.648...
5.0	−7.005 394	−12.930 16	−7.005 394	−12.930 16	−12.930 16	−266.53...	−266.528 2	−956.113...
6.0	−9.184 139	−18.006 87	−9.184 139	−18.006 87	−18.006 86	−518.04...	−518.037 4	−2079.23...

TABLE V. Zeros and poles of the clasical zeta functions in the A_1 subspace. No pole could be determined for $Z(z)$ [Eq. (1)] from the Padé approximation. (Cf. Table III.)

d/R	Z zero	ζ_0^{-1} zero	ζ_0^{-1} pole	ζ_1^{-1} zero	ζ_1^{-1} pole	ζ_2^{-1} zero	ζ_2^{-1} pole
2.5	1.617 959	1.617 959	7.095 . . .	7.095 174	15.358 . . .	15.359 95	47.27 . . .
2.8	1.963 506	1.963 506	12.181 . . .	12.180 00	28.3748 . . .	28.374 85	122.68 . . .
3.0	2.189 327	2.189 327	16.407 . . .	16.408 21	39.7475 . . .	39.747 46	206.60 . . .
4.0	3.294 206	3.294 206	48.858 . . .	48.858 24	138.153 . . .	138.153 0	1 383.5 . . .
5.0	4.382 146	4.382 146	102.44 . . .	102.439 3	327.3269	327.326 9	5 043.3 . . .
6.0	5.463 591	5.463 591	179.3 . . .	179.463 2	636.421 . . .	636.421 1	13 500 . . .

could in some cases be done with up to seven-digit precision, applying an extrapolation scheme on the results given by different orders of approximations N and L.

The improvement in the decay of the coefficients is apparent from Fig. 4, where we show the behavior of the coefficients A_n in the $P_{N-1}(z)/Q_1(z)$ approximation of the semiclassical Selberg zeta function (3); in line with the above discussion we have approximated the denominator by $Q_1(z) = 1 - z/z_1$, where z_1 is the leading zero of ζ_1^{-1}. With the leading pole gone, the faster-than-exponential decay now continues beyond $n = 4$ out to $n = 5$ or 6.

In the classical Selberg zeta function we were not able to identify any pole with the Padé technique ($N \leq 13$), which would imply that they are all canceled by zeros of higher-order dynamical zeta functions. As our numerical results show, however, the (leading) poles of the dynamical zeta functions are double; it is evident that the double zeros of ζ_1^{-2} do cancel the double poles of ζ_0^{-1}, as was also shown in the preceding section, but the poles of ζ_1^{-2} are then quadrupole and too many to be completely canceled by the triple zeros of ζ_2^{-3}. Thus one might expect the classical Selberg zeta function to have poles as well, the leading ones arising not from ζ_0^{-1} as in the semiclassical case, but from ζ_1^{-1}. Since the magnitude of these poles is rather large, we have not been able to extract them directly from a Padé approximation to $Z(z)$.

IV. REAL AND SPURIOUS ZEROS IN QUANTUM SPECTRA

As mentioned in the Introduction most calculations require the zeta functions not as functions of z but rather as functions of frequency ω and energy E or wave number k.

Consider therefore a case similar to the one above, but with "energy-dependent" coefficients $C_n = C_n(E)$. Set $a = 1$, $b = e^{-\delta}$, and replace z in Eq. (29) by e^{iE} to obtain a function

$$F(E) = \frac{1 - e^{iE}}{1 - e^{iE - \delta}} \ ; \tag{35}$$

it mimics the behavior of zeta functions in the case of a bounded system. We assume $\delta > 0$, consistent with $0 < b < a$ above. The function $F(E)$ has zeros $E_n = 2\pi n$, $n \in N$ along the real axis and poles $E_{n'} = 2\pi n' - i\delta$, $n' \in N$ along the line $\text{Im}(E) = -\delta$, defining the abscissa of absolute convergence in the complex E plane. We are interested in the properties of a finite-order expansion of F and introduce therefore a generalized function $\hat{F}(E,z)$ with the property $F(E) = \hat{F}(E,1)$,

$$\hat{F}(E,z) = \frac{1 - e^{iE}z}{1 - e^{iE - \delta}z}$$

$$= 1 - (1 - e^{-\delta})e^{iE}z - (1 - e^{-\delta})e^{-\delta}e^{2iE}z^2 - \cdots$$

$$= \sum_{n=0}^{\infty} C_n(E)z^n \ . \tag{36}$$

The expansion in z is only formal; at the end one sets $z = 1$. All results of the preceding section concerning zeros, poles, etc., can now be used, replacing z by e^{iE}, z_0 by e^{iE_0}, etc., and relating them to the complex E plane rather than the z plane. For a finite-order expansion of $F(E)$ one may therefore immediately state the following:

(i) Any truncation of the power series puts the zeros of $F(E)$ off the real axis; in the linear approximation we obtain $e^{iE} = (1 - e^{-\delta})^{-1}$, with solutions $E_n' = E_n - i\epsilon$, where

TABLE VI. Zeros and poles of the classical zeta functions in the A_2 subspace. No pole could be determined for $Z(z)$ from the Padé approximation. (Cf. Table III.)

| d/R	Z zero	ζ_0^{-1} zero	ζ_0^{-1} pole	ζ_1^{-1} zero	ζ_1^{-1} pole	ζ_2^{-1} zero	ζ_2^{-1} pole
2.5	−2.868 809	−2.868 809	−5.094 786	−5.094 784	−18.203 . . .	−18.200 26	−43.82 . . .
2.8	−4.076 735	−4.076 735	−7.564 134	−7.564 134	−38.338 . . .	−38.239 05	−102.967 . . .
3.0	−4.950 091	−4.950 091	−9.429 729	−9.429 729	−57.483 61	−57.483 60	−163.2066
4.0	−10.068 88	−10.068 88	−21.468 10	−21.468 10	−255.25 . . .	−255.258 6	−876.6592
5.0	−16.266 57	−16.266 57	−38.061 85	−38.061 86	−703.34 . . .	−703.344 5	−2785.186
6.0	−23.348 95	−23.348 95	−59.222 79	−59.222 79	−1519.21 . . .	−1519.201	−6777.36 . . .
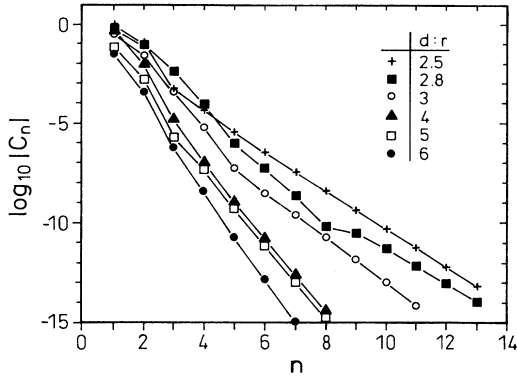
FIG. 4. Improved convergence is achieved in the semiclasical Selberg zeta function (3) after removal of the leading pole: The figure shows the expansion coefficients of $(1-z/z_1)Z(z)$, where z_1 is the leading zero of $\zeta_1^{-1}(z)$. The data are for the A_1 subspace.

$\epsilon = -\ln(1-e^{-\delta})$; for δ sufficiently large $\epsilon \approx e^{-\delta}$. The imaginary part of the energy vanishes with increasing N like $\epsilon \sim e^{-\delta N}$. Large N are required if the poles lie close to the real axis.

(ii) Ghost zeros of $F(E)$ will be found in the neighborhood of the line $\mathrm{Im}(E) = -\delta$: There are $N-1$ of them distributed more or less evenly around the circle $|e^{iE}| = e^{\delta}$, they satisfy $e^{iE} = e^{i\phi_j + \delta_j}$ with $\delta_j \approx \delta$, $0 \le \phi_j < 2\pi$, $j = 1, 2, \ldots, N-1$, i.e., $E = E_{n,j} = E_n + \phi_j - i\delta_j$. The ghost zeros converge towards the abscissa of absolute convergence and their number goes to infinity with N.

One may remove poles in the same manner as before; the formal expansion $\hat{F}(E,z) = \sum_n C_n(E) z^n$ is approximated with the Padé technique, z is set to 1, and what is left is a power-series approximation of the part of $F(E)$ containing the zeros. The energy-dependent analog of the two-pole example in the preceding section demonstrates the general tendency:

(iii) Removing leading poles has the following effect: Ghost zeros are pushed down in the negative imaginary direction; main zeros having small imaginary part approach the real axis.

The numerical investigations in this paper were performed for an open hyperbolic system, and property (i) has no relevance. Properties (ii) and (iii) are not restricted to bounded systems, though. We present numerical evidence that the removal of the leading pole does indeed push what seems to be ghost zeros in the open three-disk system far down in the negative complex energy plane: Figure 5(a) shows the lower part of the spectrum of the $N = 8$ approximation of the semiclassical Selberg zeta function together with an improved spectrum where the leading pole has been removed (Padé, $L = 1$). The original spectrum displays, in addition to the main zeros which lie relatively close to the real axis, a whole band of lower-lying zeros. When plotting spectra with higher N, one obtains main zeros at the positions of the old ones, but the zeros in the band seem not to stabilize and their number increases with N. In the improved spectrum in

Fig. 5(a) a few zeros in the band remain with approximately unchanged or even larger imaginary part, while most of the others are pushed away; in a certain range around $\mathrm{Re}(k) \approx 13$, however, no such improvement of the spectrum can be noted.

To find out whether the remaining zeros correspond to real resonances, we can compare Padé improved spectra for different N. Figure 5(b) shows improved $(L = 1)$ spectra for $N = 6$ and 8. Except for the zeros in the interval $\mathrm{Re}(k) \approx 10-16$ most remaining zeros in the $N = 8$ approximation correspond also to a nearby zero in the $N = 6$ approximation and thus seem to be stable. One exception is the zero at $k \approx 24.4 - i1.5$; we have checked with the $N = 10$ approximation though and have found a corresponding zero very close to that position.

To see the correlation between the quantum spectra in Fig. 5(a) and the position of the leading poles, we have plotted the absolute values of the two lowest zeros of $\zeta_1^{-1}(E,z)$ [assuming that they equal the poles of $\zeta_0^{-1}(E,z)$ and $Z(E,z)$] as a function of $\mathrm{Re}(k)$ with $\mathrm{Im}(k) = -2.5$ fixed; see Fig. 6. At low values of $\mathrm{Re}(k)$ the magnitude of
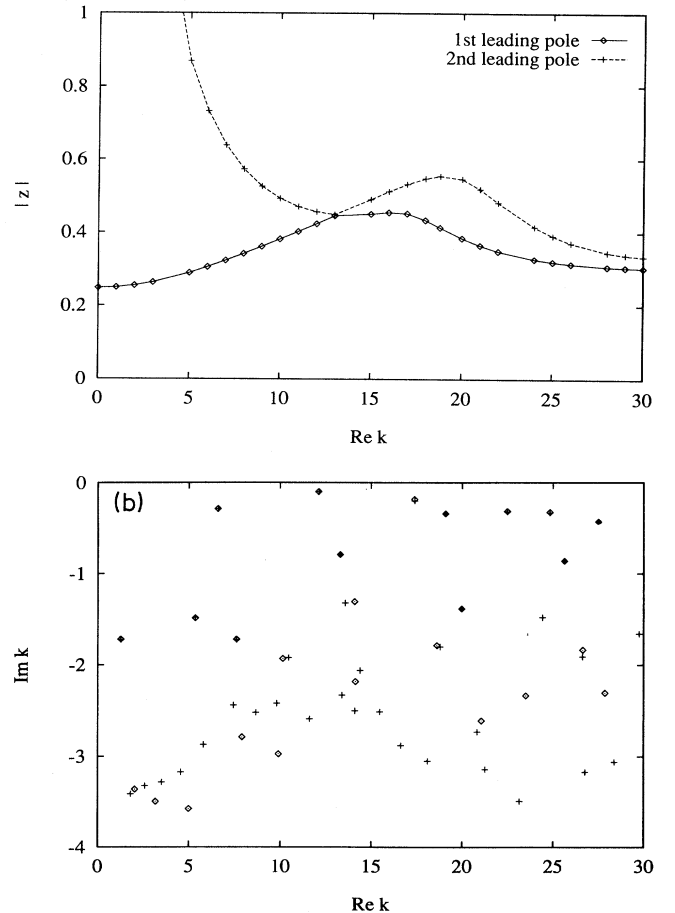

FIG. 5. Semiclassical resonances for the open three-disk system for $d/R = 3$, computed using Selberg's zeta function in the A_2 subspace. The energy is expressed in terms of $k = k(E) \equiv \sqrt{2mE}/\hbar$. (a) Spectrum in the $N = 8$ approximation, without removal (diamonds) and with removal (crosses) of the leading pole. (b) Spectrum with the leading pole removed, in the $N = 8$ (diamonds) and $N = 6$ (crosses) approximation.
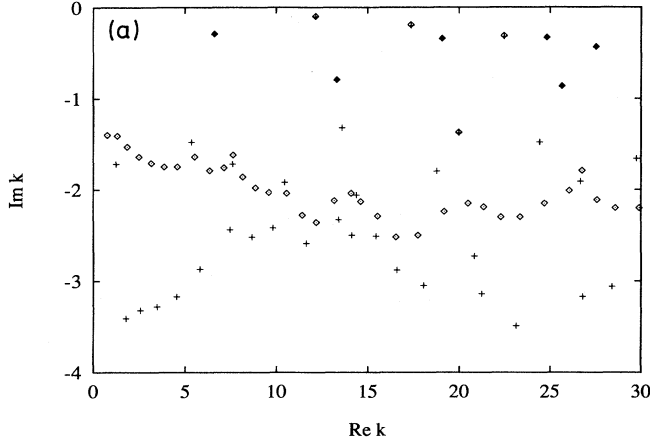
FIG. 6. The magnitude of the leading and next-to-leading zero of the semiclassical $\zeta_1^{-1}(E,z)$ as a function of $\mathrm{Re}(k)$ with $\mathrm{Im}(k) = -2.5$. The zeros are assumed to equal the leading and next-to-leading pole of $Z(E,z)$. $(d/R = 3, A_2$ subspace.)

the second pole is much larger than the leading one, so that the removal of the leading pole has a large effect on the spectrum, which is also observed in Fig. 5(a). Around $\mathrm{Re}(k) \approx 13$ the two poles are very close in magnitude, which explains why the removal of just one pole only marginally affects the spectrum. For increasing $\mathrm{Re}(k)$ the number of leading poles with comparable magnitude increases; it becomes more and more difficult to improve the spectrum.

V. SUMMARY AND DISCUSSION

We have presented numerical evidence that the semiclassical and perhaps the classical Selberg zeta functions for the open three-disk system have poles. This shows that results for 1D maps [9,26] cannot be transferred immediately to higher-dimensional systems, such as the three-disk system. In the semiclassical case it was clear already from a simple plot of the expansion coefficients that the convergence soon settles for a simple exponential decay. This was confirmed by (1) a numerical determination of zeros and poles of dynamical zeta functions, showing that the leading poles of ζ_j^{-1} equal the leading zeros of ζ_{j+1}^{-1}, but are double and therefore not completely canceled; (2) a numerical estimate of the curvature corrections of ζ_0^{-1}, showing that the leading pole is double; (3) an analysis of the explicit terms in the expansion of $Z(z)$, which with use of (2) showed that necessary cancellations between cross terms, in addition to those present within the curvatures, do not occur, causing a transition in the convergence rate at around $n = 4$; and (4) the fact that stable poles could be extracted from $Q_L(z)$, the denominator of a Padé approximation, $Z(z) \approx P_{N-L}(z)/Q_L(z)$, and that the numerator $P_{N-L}(z)$ showed improved convergence.

In the classical case, the presence of poles would be rather surprising, since the system under consideration is an almost ideal hyperbolic 2D system (complete binary symbolics, highly unstable periodic orbits with $|\Lambda_p| \gg 1$, no intermittency). Points (1)–(3) above also apply to the

classical zeta function, but we have not been able to stably identify poles from a Padé approximation. This may be due to their large imaginary parts as explained at the end of Sec. II C: The poles of ζ_0^{-1} are canceled by the zeros of ζ_1^{-1}, but there are not enough zeros from ζ_2^{-1} to cancel the poles in ζ_1^{-1}. A plot of the expansion coefficients of the classical Selberg zeta function is consistent with the anticipated, pole free $\exp\{-n^{3/2}\}$ decay (this was also found by Cvitanović and Rosenqvist [27]). One option we have not been able to test is whether the poles are in fact completely canceled by next-to-leading-order zeros of dynamical zeta functions.

Since the zeros of dynamical zeta functions are relatively easy to compute, one may also quite easily identify the poles, provided there is a 1:1 (here rather 2:1) correspondence between poles and zeros of neighboring dynamical zeta functions. Our numerical findings give evidence that this is most probably the case for the *leading* zeros and poles. With the precision of our investigations, we were not able to identify stable next to leading poles from $Q_L(z) = 0$ more than in a few cases and then only with 1–2 digits precision; in these cases there did exist a next-to-leading-zero within the uncertainty of the pole.

There are several ways to remove poles. The Padé numerator $P_M(z)$ directly gives an approximation of $Z(z)$ or $\zeta_0^{-1}(z)$. One may also first compute leading pole estimates $\tilde{z}_n$ from zeros of dynamical zeta functions and then multiply $\prod_n(1 - z/\tilde{z}_n)$ into the expansion of $Z(z)$. Furthermore, the classical Selberg zeta function can be used with semiclassical weights to improve the convergence for semiclassical zeros; the poles of ζ_0^{-1} will then be gone. If, finally, there actually is an m:1 correspondence between the poles of ζ_j^{-1} and the zeros of ζ_{j+1}^{-1} for all j, the following construction,

$$\tilde{Z}(z) \equiv \prod_j [\zeta_j^{-1}]^{m^j}(z)$$

$$= \exp\left\{ -\sum_p \sum_r \frac{z^{rn_p}}{r} \frac{t_p^r}{1 - m\Lambda_p^{-r}} \right\}, \tag{37}$$

is free of poles and has zeros which equal the zeros of $\zeta_0^{-1}(z)$ and $Z(z)$. A numerical test for the three-disk system ($m = 2$) shows that this zeta function (classical or semiclassical weights) really has faster-than-exponential convergence all the way out to the largest n considered ($= 13$). Equation (37) and related forms require further investigations.

Recently, quantum spectra of bounded chaotic systems have been computed from expansions of semiclassical Selberg zeta function [28–30]. Despite some success, the calculations were made difficult by slow convergence, no clear indication that the zeros of the Selberg zeta function approach the real axis as $N \to \infty$, missing quantum levels, and presence of spurious zeros [i.e., zeros of $Z(E)$ not associated with exact quantum eigenvalues]. The pole-induced properties (i) and (ii) of the preceding section are recognizable here. We therefore suggest a relation, similar to the simple example above, between the position of poles and the distance from the real axis of the zeros of $Z(E)$ [or $\zeta_0^{-1}(E)$] in bounded systems. In

the calculations for the anisotropic Kepler problem and the closed three-disk system, there is one obvious pole, connected with an orbit not realized by the dynamics, but for which heteroclinic orbits of arbitrary length exist. This pole has been removed in the calculations reported in [29]. But the present investigation suggests that there are further poles not so simply identified. We suspect that they are at least partially responsible for the bad convergence of the zeros of $Z(E)$ (in bounded systems there are many other sources of trouble, like intermittency and stable islands). Spurious zeros present in cycle ex-

panded spectra could be (in many cases at least) nothing but the ghost zeros connected to the poles. Improved spectra should therefore be obtained by removing the leading poles, as done here for the open three-disk system.

ACKNOWLEDGMENT

*Present address: FB8, C. v. Ossietzky Universität, Postfach 2503, 2900 Oldenburg, Germany.

[1] D. Ruelle, *Statistical Mechanics* (Addison-Wesley, Reading, MA, 1978).

[2] J. P. Eckmann and D. Ruelle, Rev. Mod. Phys. **57**, 617 (1985).

[3] R. Artuso, E. Aurell, and P. Cvitanović, Nonlinearity **3**, 325 (1990).

[4] R. Artuso, E. Aurell, and P. Cvitanović, Nonlinearity **3**, 361 (1990).

[5] P. Cvitanović and B. Eckhardt, J. Phys. A **24**, L237 (1991).

[6] B. Eckhardt, in *Quantum Chaos*, Proceedings of the International School of Physics "Enrico Fermi," Course CXIX, Varenna, 1991, edited by G. Casati, I. Guarneri, and U. Smilansky.

[7] A. Selberg, J. Indian Math. Soc. **20**, 47 (1956).

[8] N. Balazs and A. Voros, Phys. Rep. **143**, 109 (1986).

[9] F. Christiansen, P. Cvitanović, and H. H. Rugh, J. Phys. A **23**, L713 (1990).

[10] E. Aurell, J. Stat. Phys. **58**, 967 (1990).

[11] B. Eckhardt, J. Phys. A **20**, 5971 (1987).

[12] P. Gaspard and S. A. Rice, J. Chem. Phys. **90**, 2225 (1989); **20**, 2242 (1989); **20**, 2255 (1989).

[13] P. Cvitanović and B. Eckhardt, Phys. Rev. Lett. **63**, 823 (1989).

[14] B. Eckhardt, G. Russberg, P. Cvitanović, P. E. Rosenqvist, and P. Scherer, in *Quantum Chaos*, edited by

G. Casati and B. V. Chirikov (Cambridge University Press, Cambridge, England, in press).

[15] M. C. Gutzwiller, *Chaos in Classical and Quantum Mechanics* (Springer, New York, 1990).

[16] M. C. Gutzwiller, J. Math. Phys. **8**, 1979 (1967); **10**, 1004 (1969); **11**, 1791 (1970).

[17] A. Voros, J. Phys. A **21**, 685 (1988).

[18] J. Robbins, Phys. Rev. A **40**, 2128 (1989).

[19] B. Lauritzen, Phys. Rev. A **43**, 603 (1991).

[20] P. Cvitanović and B. Eckhardt, Nonlinearity (to be published).

[21] J. Plemelj, Monatsh. Math. Phys. **15**, 93 (1909).

[22] F. Smithies, Duke Math. J. **8**, 107 (1941).

[23] M. Reed and B. Simon, *Analysis of Operators*, Methods of Modern Mathematical Physics Vol. 4 (Academic, New York, 1978).

[24] E. R. Hansen, *A Table of Series and Products* (Prentice-Hall, Englewood Cliffs, NJ, 1975).

[25] G. A. Baker, *Essentials of Padé Approximants* (Academic, New York, 1975).

[26] M. Pollicott, J. Stat. Phys. **62**, 257 (1991).

[27] P. Cvitanović and P. Rosenqvist (private communication).

[28] P. Dahlqvist and G. Russberg, J. Phys. A **24**, 4763 (1991).

[29] G. Tanner, B. Scherer, E. B. Bogomolny, B. Eckhardt, and D. Wintgen, Phys. Rev. Lett. **67**, 2410 (1991).

[30] M. Sieber and F. Steiner, Phys. Rev. Lett. **67**, 1941 (1991).